Epilepsia, 54(8):1391–1401, 2013
doi: 10.1111/epi.12202

FULL-LENGTH ORIGINAL RESEARCH

Potential for unreliable interpretation of EEG recorded with microelectrodes

*†William C. Stacey, ‡Spencer Kellis, §Bradley Greger, ¶Christopher R. Butson, †Paras R. Patel, #Trevor Assaf, *Temenuzhka Mihaylova, and *Simon Glynn

*Department of Neurology, University of Michigan, Ann Arbor, Michigan, U.S.A.; †Department of Biomedical Engineering, University of Michigan, Ann Arbor, Michigan, U.S.A.; ‡Division of Biology, California Institute of Technology, Pasadena, California, U.S.A.; §Department of Bioengineering, University of Utah, Salt Lake City, Utah, U.S.A.; ¶Departments of Neurology and Neurosurgery, Medical College of Wisconsin, Milwaukee, Wisconsin, U.S.A.; and #Department of Computer Science, University of Michigan, Ann Arbor, Michigan, U.S.A.

Summary

Purpose: Recent studies in epilepsy, cognition, and brain machine interfaces have shown the utility of recording intracranial electroencephalography (iEEG) with greater spatial resolution. Many of these studies utilize microelectrodes connected to specialized amplifiers that are optimized for such recordings. We recently measured the impedances of several commercial microelectrodes and demonstrated that they will distort iEEG signals if connected to clinical EEG amplifiers commonly used in most centers. In this study we demonstrate the clinical implications of this effect and identify some of the potential difficulties in using microelectrodes.

Methods: Human iEEG data were digitally filtered to simulate the signal recorded by a hybrid grid (two macroelectrodes and eight microelectrodes) connected to a standard EEG amplifier. The filtered iEEG data were read by three trained epileptologists, and high frequency oscillations (HFOs) were detected with a well-known algorithm. The filtering method was verified experimentally by recording an injected EEG signal in a saline bath with the same physical acquisition system used to generate the model. Several electrodes underwent scanning electron microscopy (SEM).

Key Findings: Macroelectrode recordings were unaltered compared to the source iEEG signal, but microelectrodes attenuated low frequencies. The attenuated signals were difficult to interpret: all three clinicians changed their clinical scoring of slowing and seizures when presented with the same data recorded on different sized electrodes. The HFO detection algorithm was oversensitive with microelectrodes, classifying many more HFOs than when the same data were recorded with macroelectrodes. In addition, during experimental recordings the microelectrodes produced much greater noise as well as large baseline fluctuations, creating sharply contoured transients, and superimposed "false" HFOs. SEM of these microelectrodes demonstrated marked variability in exposed electrode surface area, lead fractures, and sharp edges.

Significance: Microelectrodes should not be used with low impedance (<1 GΩ) amplifiers due to severe signal attenuation and variability that changes clinical interpretations. The current method of preparing microelectrodes can leave sharp edges and nonuniform amounts of exposed wire. Even when recorded with higher impedance amplifiers, microelectrode data are highly prone to artifacts that are difficult to interpret. Great care must be taken when analyzing iEEG from high impedance microelectrodes.

KEY WORDS: Electrodes, Impedance, High frequency oscillations, Electrocorticography.

Many neurologists and neuroscientists have begun to monitor intracranial electroencephalography (iEEG) with smaller electrodes to achieve greater spatial resolution than is present in standard iEEG. These "microelectrodes" are designed to record neurophysiologic phenomena that occur on a small spatial scale. Over the past decade, two types of microelectrodes have been used. One type is a rigid, penetrating microelectrode array (MEA), which was originally designed as a brain–computer interface (BCI; Normann, 2007). This device has been used in several BCI applications such as restoring motor function in tetraplegia (Hochberg et al., 2006) and sight restoration (Davis et al., 2012). In epilepsy, MEAs have been used to record individual neuronal firing during seizures (Schevon et al., 2010; Truccolo et al., 2011), and have identified high frequency oscillations (HFOs) and microseizures (Schevon et al., 2009, 2012) that

Accepted March 21, 2013; Early View publication May 3, 2013.
Address correspondence to William Stacey, Department of Neurology, University of Michigan, 1500 E. Medical Center Drive, SPC 5036, Ann Arbor, MI 48109-5036, U.S.A. E-mail: william.stacey@umich.edu

Wiley Periodicals, Inc.

were not visible on standard EEG. Another microelectrode strategy involves using pliable 40-μm wires, and either attaching them to the substrate of standard iEEG electrodes (Van Gompel et al., 2008) or extruding them as loose wires from the end of clinical depth electrodes (Quiroga et al., 2005). These wires have recorded such behaviors as specific hippocampal cell firing (Quiroga et al., 2005), correlation between brain regions during different brain states (Le Van Quyen et al., 2010), HFOs in human epilepsy (Bragin et al., 2002), and microseizures (Stead et al., 2010). Although regular iEEG electrodes are capable of recording some of these activities (Chatillon et al., 2011), it is clear that microelectrodes have opened a new chapter in neurophysiology.

The traditional "macroelectrodes" that defined clinical neurophysiology for over half a century are spaced 1 cm apart and have exposed metal surfaces of approximately 4 mm. Clinical EEG acquisition systems were built to accommodate these electrodes, utilizing amplifiers that have electrical impedance (10–50 MΩ) that is high relative to the macroelectrodes (approximately 10 kΩ at 20 Hz; Stacey et al., 2012), thereby ensuring that the input signal is not distorted. Microelectrodes, on the other hand, have much smaller exposed surface area and their impedance is markedly higher (>1 MΩ at 20 Hz, with high variability). The examples cited in the preceding paragraph were recorded using microelectrodes connected to specialized, very high impedance acquisition systems, so that the recorded signals were not distorted. However, microelectrodes are now produced in a configuration that encourages clinicians to connect them directly to standard iEEG acquisition systems. Two major U.S. electrode manufacturers have acquired U.S. Food and Drug Administration (FDA) approval and have been marketing them to clinicians and researchers (Ad-tech Medical Instrument Corporation [Racine, WI, U.S.A.], PMT Corporation [Chanhassen, MN, U.S.A.]). This practice could lead to complications: we recently measured the impedances of macroelectrodes and microelectrodes, and predicted that macroelectrodes work very well with 10–50 MΩ amplifiers (a common input impedance on intracranial amplifiers), but that microelectrodes using these same amplifiers will attenuate low frequencies and distort signals (Stacey et al., 2012). Those findings were very reassuring for clinicians using macroelectrodes: the data predicted that the recorded signals are essentially identical to the original voltages in the brain. Microelectrodes, however, would likely not function well if connected to such a clinical system. In the current work, we demonstrate this effect on human iEEG recordings and determine its clinical implications. Our findings suggest that the very high and markedly variable impedance of microelectrodes make them ill-suited for use in most clinical EEG systems, which typically have low impedance. Connecting microelectrodes to such systems distorts the recorded EEG signals, which can lead to errors in clinical analysis.

Methods

In this work we use as baseline signals human iEEG that were originally recorded with macroelectrodes, and manipulate them to test how they would have appeared if recorded with microelectrodes. First, we inject 30 s of iEEG data into a saline bath while recording with hybrid electrodes on a clinical system to validate our simulation method. We then use the simulation to filter 200 s of iEEG data to represent how it would appear if recorded by several different electrodes.

iEEG recordings

Two samples of human iEEG were acquired from the International EEG database (https://www.ieeg.org, Study 034, Fig. S1), an open internet database of de-identified iEEG. Each EEG was a 200-s sample from seven channels recorded on standard macroelectrodes. The data were originally acquired with a Digital Lynx Data Acquisition System (Neuralynx, Bozeman, MT, U.S.A.) at 32 kHz with an input impedance of 1 TΩ. The data were then down-sampled to 5 kHz. Both samples include focal theta and delta slowing, epileptic spikes, HFOs, and one seizure.

Electrode filtering

We filtered the iEEG signals using the process described previously (Stacey et al., 2012). In summary, we first assumed that the raw macroelectrode iEEG data were the gold standard, representing the true cerebral signal to which all data were compared. This assumption is supported by the results of that article, which showed that macroelectrodes in typical clinical systems produce negligible distortion of the original brain signal. We then filtered this signal using transfer functions that replicate the distortion caused by the electrode impedances, which were measured previously. This method was necessary to ensure that all electrodes received identical input under all conditions. In general, if the electrode impedance is small in comparison to the input impedance in the amplifier, the distortion is negligible. Conversely, the greatest distortion occurs when high impedance electrodes (microelectrodes) are connected to low impedance amplifiers used in typical iEEG acquisition systems.

Experimental recordings

We performed an experimental recording using standard EEG equipment to verify the filtering effects that were predicted by the mathematical method described above (see Fig. 1A). We connected an Ad-tech hybrid iEEG grid (2 macro × 8 micro contacts) to a Neurolink IP64 amplifier and recorded at 1,024 Hz using NeuroWorks software (Natus Medical, San Carlos, CA, U.S.A.), a widely used clinical EEG acquisition system and recording format. The grid was placed into a solution of 1× phosphate-buffered saline (PBS; Fisher, Hampton, NH, U.S.A.). The reference and ground connections were

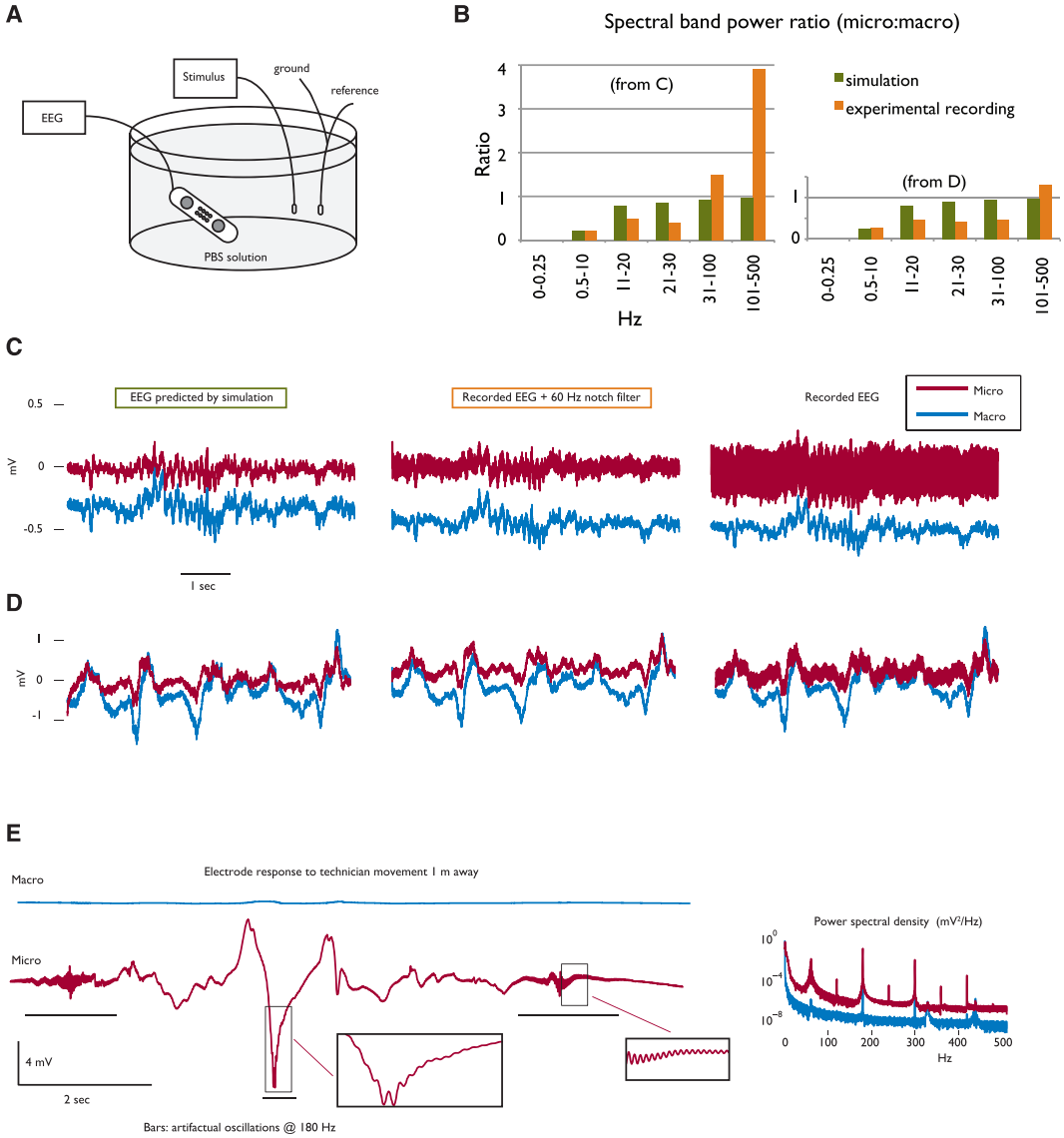

Figure 1.
Experimental recording. (**A**) Diagram of experimental set up. An Ad-tech hybrid grid was connected to a Neurolink IP64 head box and recorded with Natus Neuroworks software. A stimulating electrode injected human EEG signals into the bath. Ground and reference were placed in the bath far from the stimulating electrode. (**B**) Ratio of spectral band power (microelectrode:macroelectrode) in several frequency bands for the experiment (orange), compared with the predictions from the simulation (green). (**C**, **D**) Examples of data from macro (blue) and micro (red) electrodes, comparing the simulation (left) with the experiment (center, right). A 60-Hz notch filter did not remove all noise on the micros, leaving low amplitude, high frequency noise (center). Data shown are 5-s excerpts of the 30 s datasets used in (**B**). (**E**) Artifact caused by movement near the electrodes (electrodes and wires did not move). Bars, insets: After 60-Hz notch filtering, artifactual 180 Hz oscillations were present in the micros, preferentially on fast transients. Right: Power spectral density of entire experiment after notch filtering (59–61 Hz). Noise produces broad-spectrum artifacts surrounding 60 Hz and its odd harmonics in the micros.

connected to standard copper EEG electrodes, which were also placed into the solution. This configuration approximates typical EEG wiring in a clinical setting (in our laboratory, ground is connected to the skin on the top of the head, and the reference is either one of the implanted macroelectrodes or a midline surface electrode). To validate this set up, we verified that the macroelectrode recordings had little noise and good signal fidelity (Fig. 1). Two 30-s excerpts from one channel of one of the human iEEG samples described above were used as

stimuli. The stimuli were sent to an NI 9263 analog output device through Labview software (National Instruments, Austin, TX, U.S.A.) and injected into the bath using a 22 AWG tinned copper wire (General Cable, Highland Heights, KY, U.S.A.). Data were recorded from the hybrid grid using NeuroWorks software, and then exported into text files for analysis in Matlab (Mathworks, Natick, MA, U.S.A.).

We used the signal recorded by macroelectrodes as the gold standard, as we have previously demonstrated that macroelectrodes attenuate the signal minimally (Stacey et al., 2012), and the stimulation apparatus would not necessarily deliver the precise signal it had as input. The grid was oriented orthogonal to the electrode injecting the signal, and the amplitude of the recorded signal on the two macroelectrodes was compared to account for any spatial attenuation. We found minimal difference in the amplitudes at the two macroelectrodes, and since the micro array was between them we assumed each microelectrode received identical input. We measured the spectral content of each 30 s-long recorded signal in several frequency bands by integrating the power spectral density between given frequencies, and then we computed the ratio of the power in the microelectrode recording to that of the macroelectrode (Stacey et al., 2012). This ratio therefore compares the spectral content of the microelectrode with the gold standard.

Clinical evaluation

In order to test how microelectrode recordings affect clinical interpretation, three neurologists with subspecialty training in epilepsy interpreted the iEEG sample under different scenarios. The original 200-s, seven-channel EEG signal was filtered to represent how it would have appeared if it were recorded by either (1) seven identical macroelectrodes; or seven identical microelectrodes with (2) high or (3) medium impedance. The electrode impedances were the actual measured values from three of the electrodes (one macroelectrodes, two microelectrodes) on the hybrid grid from the previous section. In each instance, filtering was calculated with the electrodes connected to an amplifier with input impedance of 10 MΩ in parallel with 8 pF, which is the specification for the Natus NeuroLink IP64 and is typical of the majority of clinical iEEG acquisition systems. The impedance measurements and filtering method were identical to our previous work (Stacey et al., 2012). All seven channels were filtered equally in each scenario, and each of the three scenarios was independent.

Clinical data

Two seven-channel iEEG samples of 200 s each were reviewed. Each sample was reviewed three separate times, using filtered datasets corresponding to how the data would appear if they were recorded with either macroelectrodes ("Macro"), high impedance microelectrodes ("micro1"), or medium impedance micros ("micro2"). There were thus a total of six datasets for review, three for each iEEG sample. In each scenario, the clinicians marked the time of seizure onset and seizure offset in every channel, using their individual clinical judgment. Seizure onset and offset times were scored for each channel individually, but in the context of the activity of the other channels. To score slow activity, reviewers looked at 10-s intervals and determined whether each channel independently had theta (4–8 Hz) and/or delta (0–4 Hz) slowing during that interval.

Interrater variability in scoring clinical EEG records is high (Brown et al., 2007; Benbadis et al., 2009). Therefore, to calculate how microelectrodes affected an individual reviewer's clinical interpretation, for each reviewer we compared the difference between their marks using the macroelectrode versus each microelectrode scenario. For seizures, we report the mean and standard deviation of the difference of onset times marked in the microelectrodes from those in the macroelectrodes for each reviewer individually. For slowing, we compare the total number of epochs to the macroelectrode scenario. For an objective comparison of slowing, we also calculated the spectral band power of each scenario by integrating the power spectral density of the entire signal in the delta (0.5–4 Hz) and theta (4.5–8 Hz) bands. After marking the studies independently, the reviewers met to determine a consensus for the earliest electrographic change (EEC) and unequivocal electrographic onset (UEO) of each seizure in the macroelectrode data (Wong et al., 2007), which was used for display purposes and normalization.

Results

Experimental validation of electrode filtering method

In our previous work, we measured hybrid macroelectrode and microelectrode impedances and used engineering methods to predict how they would filter iEEG signals when connected to several commercial amplifiers (Stacey et al., 2012). Here we validate this method experimentally by connecting a hybrid grid to the clinical iEEG acquisition system used at our hospital (Natus Neurolink IP64, input resistance 10 MΩ).

We injected two signals: one primarily with delta frequencies (<4 Hz) and another with frequencies up to the beta range (approximately 20 Hz). The simulation (Fig. 1C,D, left) predicted that the macroelectrode will not distort the signal at all—the input signal (not shown) was indistinguishable from the blue line—but the microelectrode will remove all direct current (DC) bias and distort the slower frequencies. The experimental recording showed similar results, although there was a considerable amount of noise on the microelectrode (see next section). Figure 1B quantifies the microelectrode attenuation (microelectrode spectral band power normalized to that of the macroelectrode) to compare the simulation to the experiment. In this configuration, a ratio of 1 indicates that the

microelectrode contained the same spectral power as the macroelectrode recording, and comparing the ratio of experiment to simulation indicates how well the simulation predicted the actual recording. For 0.5–10 Hz, the experiment had essentially the same spectral content as in the simulation. Of interest, for very low (0–0.5 Hz) and faster (11–30 Hz) frequencies, the experimental recording was worse than predicted. This difference is possibly due to small changes in impedance from the original measurements or to variation in the impedance of the recording amplifier from its published specifications.

Increased noise in microelectrodes

A second important effect seen in the experimental microelectrode recordings is a dramatic increase in noise. Noise was not included in the simulation. In this experiment, as in a clinical scenario, noise comes from many sources, and it is complex and difficult to predict. Except for using the PBS bath as our conducting medium, the EEG set up for the experiment was identical to that used with a patient, using the same cables and hardware. In clinical EEG recordings, the subject is isolated from true ground for safety reasons, instead using an "isolated common" electrode that is only capacitively coupled to ground, thereby minimizing 60 Hz noise. As well, both the reference and common electrodes are usually located on the head in clinical EEG recordings, to minimize 60 Hz common-mode noise sources, as well as physiologic noise from cardiac sources. We used a similar set up for our experiment.

As seen in Figure 1C,D (right), the higher impedance microelectrode is extraordinarily sensitive to external noise compared with the macroelectrode, which had negligible noise under identical conditions. Three types of noise were present in the microelectrode data. First, 60 Hz line noise was present. Analysis of the power spectral density revealed that this noise was not completely abolished by a notch filter, with significant power in frequencies surrounding 60 Hz and in the odd harmonics of 60 Hz (Fig. 1E, right). This noise was so strong in the microelectrodes that the band power >30 Hz was higher than the original signal, greatly diminishing signal to noise ratio. Second, large fluctuations in voltage occurred whenever there was movement by the experimenters within 1 m of any portion of the cable or head box (Fig. 1E, left). This movement produced trivial fluctuations on macroelectrodes, but large deflections on high impedance electrodes time-locked to the movement. Depending on the movement speed, these deflections were often similar in morphology to slow waves, sharp transients, or even epileptiform discharges. Complicating this interpretation, line noise was much more prominent on the peaks of the movement artifacts. This third noise effect was not completely removed by implementing the 60-Hz notch filter: the harmonics at 180 Hz were still quite prominent (Fig. 1E, left). This resulted in 180-Hz sinusoidal noise that occurred preferentially on the peaks of transients. This noise could be easily mistaken for physiologic HFOs: it is a 180-Hz oscillation that rides on activity similar to sharp waves. Great care must be taken to distinguish such artifacts from physiologic HFOs (Worrell et al., 2012).

SEM imaging of microelectrodes

We previously measured dramatic differences in microelectrode impedance, up to three orders of magnitude in neighboring electrodes (Stacey et al., 2012). Here we investigate this disparity using SEM. Given that all electrodes are made of the same material, the exposed surface area plays a major role in determining impedance. Microelectrodes are manufactured by anchoring 40-μm wires into the silastic substrate of the electrode grid. There is a small difference between the two electrode brands we tested: PMT microelectrodes are placed in a pillar of silastic that rises out of the flat substrate, whereas the Ad-tech version contains no pillar. There was no appreciable difference in impedance distributions between these two electrode types in our previous measurements (Stacey et al., 2012). As seen in Figure 2, we imaged 80 of the microelectrodes from that paper and correlated their SEM images with the impedances (all impedances listed refer to the measured magnitude at 20 Hz). We found that the very high and very low impedances were clearly associated with surface area of the wire. For instance, the two highest impedance electrodes (8.1 and 7.6 MΩ) were the two that had the most insulation covering the wire tip, and all electrodes with torn insulation exposing the wire shaft had low impedance (<100 kΩ; Fig. 2A). However, visual inspection was not sufficient for all cases: many electrodes with similar appearance had impedances ranging from 200 kΩ to 6 MΩ. There were other irregularities as well: the condition and positioning of the electrodes within the silastic substrate was not uniform; and there were occasional sharp, ragged edges or fractures in the wires. The clinical implications of these latter findings are unclear, as these electrodes are only 40-μm wide and it is known that even conventional macroelectrodes are not innocuous to brain tissue. However, these findings suggest that some microelectrodes may not be as innocuous as clinicians hoped, particularly if the grid moves when these electrodes are in direct contact with the brain surface.

Clinical interpretation of microelectrode recordings

Using the method previously described (Stacey et al., 2012), we filtered seven channels of human iEEG to represent how the recordings would have looked if recorded by (1) a macroelectrode or a microelectrode with either (2) high or (3) medium impedance. The three electrode impedances used were taken from actual impedance measurements on the grid used in the experiment above. Two seizures recorded on iEEG data samples of 200 s each were used, resulting in six total scenarios presented to each clinician, as if each seizure were recorded with either a macroelectrode, a high impedance microelectrode, or a medium impedance

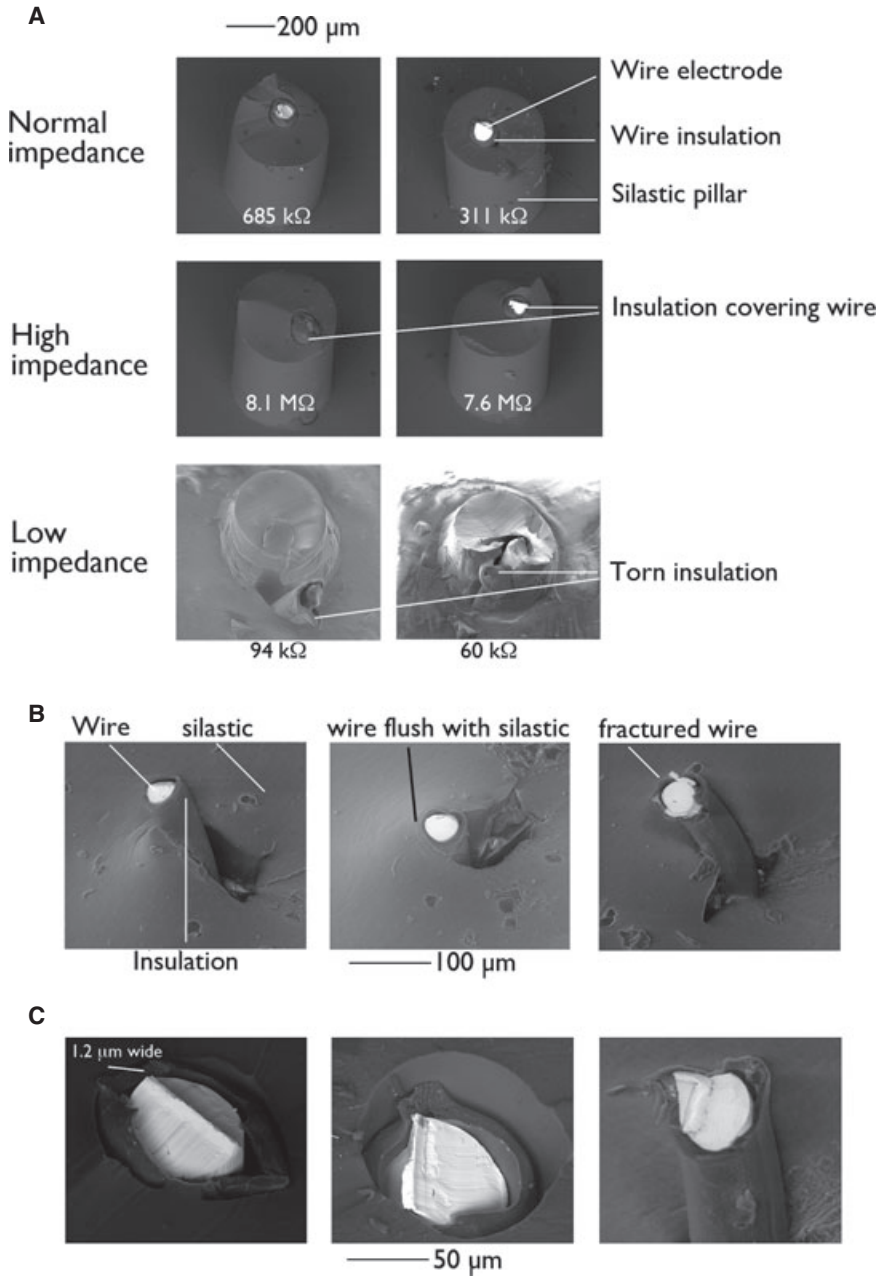

Figure 2.
SEM of microelectrodes. (**A**) Scanning electron microscopy of PMT microelectrodes. The 40-µm wires are embedded in silastic pillars. Top: typical appearance showing exposed metal wire tip. Impedances (magnitude at 20 Hz) ranged from 200 kΩ to 5 MΩ. Text shows measured impedance for indicated electrode. Middle: the highest impedances occurred when insulation covered the wire tip, minimizing surface area. Bottom: electrodes with torn insulation had more exposed surface area and much smaller impedance. The electrodes are also not centered in the silastic pillar. (**B**) SEM of Ad-tech microelectrodes. Left: typical appearance of 40-µm wire extruding from the silastic backing. Middle: very short wire unlikely to contact tissue. Right: example of irregular, fractured edge. (**C**) Sharp and irregular edges were present from both manufacturers (Left/middle: PMT. Right: Ad-tech).

microelectrode using routine clinical iEEG acquisition systems. As seen in Figure 3, microelectrodes distort the original signal significantly when using typical clinical amplifiers; however, this distortion is eliminated if high input impedance amplifiers are used. This distinction is critical: to our knowledge all published data using microelectrodes have used appropriate, high impedance amplifiers (≥ 1 TΩ), and thus this signal distortion would not be seen in those data. Conversely, the results that follow demonstrate the effect of using high impedance microelectrodes on the amplifiers that are typically present in clinical iEEG acquisition systems in major epilepsy centers.

In this analysis, we did not assume that any particular signal or interpretation was right or wrong; rather, each reviewer's ratings with microelectrodes were compared with their own judgment on the macroelectrode data. Clinical assessment of delta and theta slowing were both greatly affected by microelectrodes (Fig. 4A,B). Delta slowing in particular was nearly abolished in the high impedance microelectrode. This change in clinical scoring was proportional to the attenuation of band power. Clinical scoring of theta slowing was similar, although there was some variability among the reviewers and one felt that theta slowing was more prominent in the microelectrode recording.

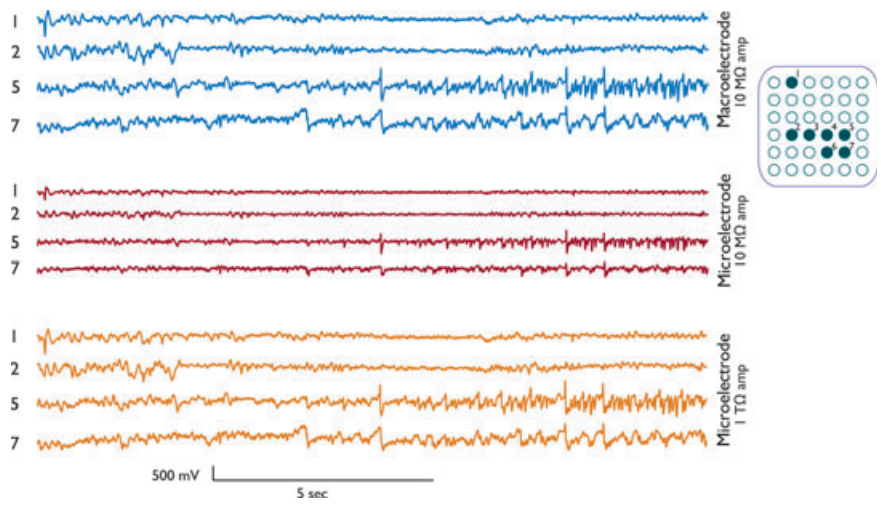

Figure 3.
Attenuated EEG with microelectrodes. Human EEG data were filtered to simulate the attenuation produced when recorded with macro (top, blue) and micro (middle, red) electrodes on a typical clinical amplifier (10 MΩ). The source data are identical to the blue signal at top because there is negligible distortion with macroelectrodes. The microelectrode severely distorts the lower frequencies. This distortion can be avoided if recorded on a high impedance amplifier, such as this 1 TΩ example (bottom, orange). Right: schematic of the 8 × 8 grid used in the original recording. The labeled electrodes 1–7 were all included in the EEGs shown to clinicians in Figure 4.

Determination of the timing and location of seizure onset is the most critical aspect of interpreting clinical intracranial recordings, and these also were disrupted in the microelectrode recordings. When normalized to the consensus earliest electrographic change (EEC; Fig. 4C,D), seizure onset times determined by each reviewer were similar, but all three reviewers changed the onset time in at least one channel by up to 10 s (Table 1). An example of the scoring for each reviewer of seizure onset time in one particular channel is shown in Figure 4F. Localization of the seizure onset was also disturbed (Fig. 4E). All three reviewers changed their localization when microelectrodes were used, and in some cases also changed the extent of involved tissue (false positives, Table 1). Both of these effects obviously could have important clinical consequences.

Automated HFO detection overestimated with microelectrodes

The iEEG dataset above is notable because of frequent HFOs in two of the channels, especially during the patient's seizures. These data were used previously in a large analysis of the relationship between HFOs and the seizure-onset zone (Blanco et al., 2010, 2011) that was based upon a well-known automated HFO detector (Staba et al., 2002). We used the same HFO detector to process the three filtered EEG datasets described above, in order to demonstrate how the analysis would change if the data had been acquired with the microelectrodes on a 10-MΩ acquisition system. As seen in Figure 5, signals recorded from higher impedance microelectrodes on 10-MΩ amplifiers cause the automated detector to overestimate the number of HFOs. This somewhat counterintuitive result occurs because the algorithm normalizes the potential HFOs to the background power, which is attenuated in high impedance electrode recordings. Therefore, more putative HFOs are identified with higher impedance electrodes, many of which are false positives, since the algorithm was originally tuned to nonattenuated data (Staba et al., 2002). Note that this effect does not refute past research about HFOs that used microelectrodes with ≥ 1 TΩ amplifiers: it only occurs when microelectrodes are connected to traditional low impedance (≤ 100 MΩ) amplifiers. Therefore, previous work utilizing high impedance amplifiers (e.g., Schevon et al., 2009; Stead et al., 2010; Truccolo et al., 2011) does not reflect this bias.

Discussion

Clinical consequences of microelectrode recordings

Microelectrodes are FDA approved and can be added to standard iEEG grids. They are integrated into the standard pigtail connectors and are convenient to connect to existing EEG head box amplifiers. In this work, we have not addressed the differences in spatial resolution that separate microelectrodes and macroelectrodes. The disparities we identify are due to the fact that most clinical EEG amplifiers were not designed for use with the very high impedances present in microelectrodes. This impedance imbalance attenuates the low frequency components of the recorded

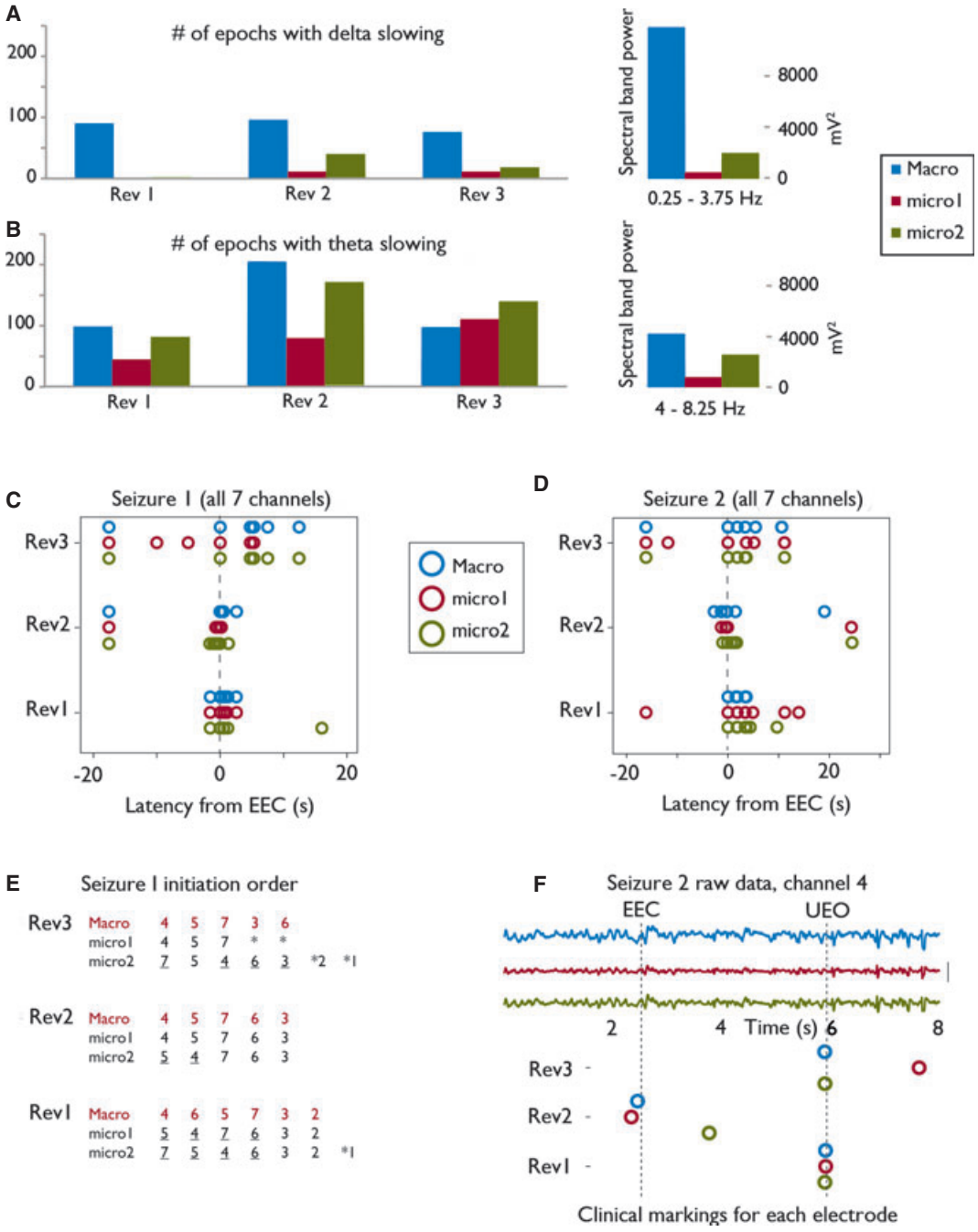

Figure 4.

Clinical interpretation disrupted with microelectrodes. A seven-lead EEG was filtered three separate times to simulate recording with a macro (blue) and two micro (red, green) electrodes. Three clinicians reviewed the EEG to identify seizures and slowing. (**A**, **B**) Left: Total number of 10-s epochs deemed to contain delta (**A**) or theta (**B**) slowing. Microelectrodes underestimated delta slowing for all three reviewers, and theta in two of three reviewers. Right: quantitative measurement of total band power in delta and theta range. These ratios are similar to the clinical markings. (**C**, **D**) Seizure onset time in each of the seven leads for two different seizures, normalized to the earliest electrographic change (EEC). When the same seizure was viewed from microelectrodes, each reviewer changed the onset time of at least one electrode by up to 10 s, and two reviewers labeled false-positive onset times (see Table 1). (**E**) All three reviewers determined that seizure onset occurred on different leads with microelectrodes (underlines), and two changed the extent of seizure spread (asterisks). (**F**) An example of the raw data from lead four recorded by all three electrodes, with each reviewer's markings underneath. EEC and UEO were determined by post hoc consensus.

Table 1. Clinical scoring, seizure onsets

	Mean	SD	Range	False positives
Micro1	−0.8	2.5	−10.4–3.1	4/14
Micro2	−0.6	2.4	−10.4–2.2	5/14

Each clinician's seizure-onset markings for the two microelectrodes were normalized to their own markings on the macroelectrode data. The mean, standard deviation (SD), and range were calculated from the normalized seizure onset time (in s) from each reviewer, pooled together. False positives indicate the total number of channels incorrectly identified as being involved in the seizure out of the total of 14 channels (see Fig. 4E).

signal. We demonstrate that this attenuation has several disruptive effects on EEG interpretation.

Identification of EEG phenomena depends upon complex visual processing of a wide range of frequencies. Some waveforms contain primarily high frequencies, notably fast ripples (>200 Hz) and multiunits (>1,000 Hz). These phenomena are not affected by the attenuation due to the frequency response of the microelectrodes (Stacey et al., 2012). However, most other waveforms, especially those that comprise clinical EEG interpretation, have important slow frequency components <100 Hz. Asymmetric attenuation of some of these frequencies distorts the signal. The most straightforward effect is the loss of slow activity that indicates cerebral dysfunction. But it also has more complex effects. For instance, a classical epileptic spike is a sharp peak followed by a slow wave. When the slow wave is removed, the spike becomes difficult to interpret. This effect can be problematic when evaluating the runs of spikes during a seizure, as seen in Figures 3 and 4. Given the nuances that comprise clinical interpretation, any distortion of the signal complicates interpretation and introduces uncertainties, especially the large effects seen in these examples. In our opinion, microelectrodes are not suitable for use in iEEG acquisition systems with impedance ≤ 100 MΩ. We previously predicted that amplifiers should have an impedance of at least 1 GΩ to be used with microelectrodes (Stacey et al., 2012). These data predict that the microelectrode recordings with high impedance systems will represent the original signal very well.

In addition, our data show that macroelectrodes have excellent signal fidelity for the full frequency range: the recorded EEG is essentially identical to the voltage present at the electrode tip. This relationship depends only upon impedance, and should hold true for all macroelectrodes with similar materials and surface area, even different shapes such as depth macroelectrodes.

Increased noise in microelectrodes

Our validation experiment demonstrates a second difficulty using high impedance microelectrodes: dramatic increases in noise. This effect was not due to thermal or 1/f noise, which are low amplitude and have a broad power spectrum (McAdams et al., 2006). Rather, the noise is centered near odd harmonics of 60 Hz with a wide dispersion,

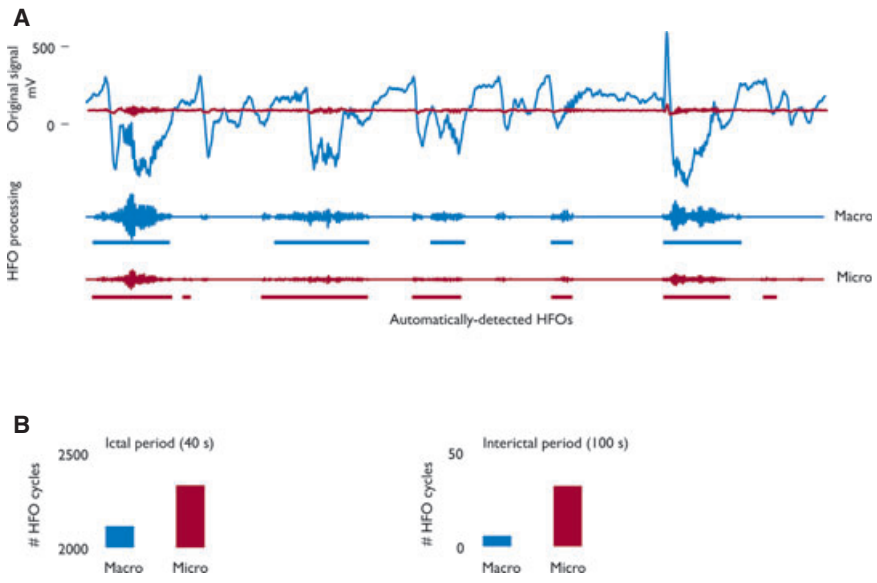

Figure 5.
Automated HFO detection disrupted by microelectrodes. (**A**) Top: Raw data from macro (blue) and micro (red) electrodes show how the higher frequency HFOs are preserved despite severe attenuation of the lower EEG signals. Bottom: After processing to maintain only 100–500 Hz signals that are significantly above baseline (Staba et al., 2002), HFOs are detected when there are more than six oscillations. Because the baseline is so attenuated in the micros, this ratio often overestimates the number of HFOs. (**B**) Count of the total number of oscillations during one ictal and interictal period. The microelectrode "detects" many more oscillations.
Epilepsia © ILAE

suggesting frequency distortion and clipping from oversaturated amplifiers (Lathi, 2005). Because of the strong harmonics and the broad spectral peak, a notch filter is not able to remove the 60 Hz noise or its harmonics adequately. This problem is independent of the amplifier impedance. Better electrical shielding or use of high impedance preamplifier "buffers" would be helpful, but are not part of most clinical procedures or hardware. An alternative is to filter higher frequencies. This is done automatically by some EEG viewing software packages (for instance, the high frequency noise seen in Figure 1 was not visible when displayed in Natus Neuroworks, even with filters "off"), but this would remove other high frequencies of interest as well, such as HFOs.

The very high impedance of the microelectrodes also results in large fluctuations in the baseline voltage due to movement artifact. In our experiment, these artifacts were induced at a distance of up to 1 m with the recording apparatus completely immobile; in a clinical scenario the patient would be moving, and this artifact could be even more prominent. Clinicians usually can identify movement artifacts, but they greatly disrupt interpretation. Furthermore, in our experiment we demonstrate that microelectrode artifacts have some properties that are unfamiliar to most clinicians, such as occurring only on select electrodes or having the appearance of physiologic HFOs. All of these noise effects are proportional to the electrode impedance, but unlike the attenuation of low frequencies described earlier, are not eliminated by using high impedance amplifiers. Similar movement artifacts are present in clinical human microelectrode recordings using a 1 TΩ Neuralynx device (Fig. S1). Alternative strategies are necessary to reduce the 60 Hz noise and motion artifacts. One solution is to use different placement and routing of reference and ground to maximize the common mode rejection at the amplifiers. In our experience with nonhuman primates and human patients, noise can be minimized by placing a buffering preamplifier on the head, very close to the electrode itself. Although these strategies have been successful in experimental studies, they will be difficult to implement in most clinical centers as they require specialized equipment and training of personnel. Another solution is to develop lower impedance microelectrodes, but these are not yet available. One interesting possibility is to take advantage of the fact that microelectrodes with less insulation at the tip (Fig. 2A) have fairly low impedances (about 50–100 MΩ, compared with 2–10 kΩ in macroelectrodes). As shown in Figure 1, low impedance electrodes are less susceptible to noise, suggesting that new manufacturing techniques that expose more of the 40-μm wire may help reduce noise. Therefore, accurate implementation of high impedance microelectrodes in patients is dependent upon carefully choosing and configuring clinical technology: high impedance amplifiers are necessary to improve signal fidelity, and better strategies are needed to reduce noise.

Conclusion

Recording iEEG with microelectrodes has yielded some important results, and is based on compelling physiologic rationale. It is important to note that our recommendations for microelectrodes do not refute past research; rather, they serve as a guideline and a warning for those who wish to begin using microelectrodes in the clinical setting. Because of their size, microelectrodes have much higher impedance than macroelectrodes. Variability in manufacturing, apparent on SEM images, explains why impedance can vary so widely among microelectrodes. If used with clinical iEEG acquisition systems, which were not designed to accommodate such high impedances, microelectrodes will yield distorted signals that complicate clinical interpretation. This attenuation can be avoided by using amplifiers with >1 GΩ input resistance—which is what previous studies have utilized. However, under typical clinical conditions, increased noise will be present on microelectrodes even when recorded with high impedance amplifiers. This noise can be disruptive to clinical interpretation, especially when it has the appearance of physiologic waveforms. The effects of attenuation and noise are both especially problematic when analyzing HFOs, as they disrupt detection algorithms and produce artifactual oscillations.

Producing accurate, reliable recordings with microelectrodes requires attention to all aspects of the acquisition system: electrodes, wire placement, amplifier placement, and impedance. Much of the necessary technology already exists, but implementing any of these procedures requires considerable investment in hardware, training, and personnel. We hope that in the near future technologies such as high impedance amplifiers and safe, low impedance microelectrodes will be more readily available to allow more centers to adopt this exciting clinical and research tool. We recommend that those interested in using microelectrodes carefully consider these potential confounding effects prior to implementation.

Acknowledgments

This work was supported by the National Institutes of Health (K08NS069783 to WS) and a Utah Research Foundation grant to BG. The authors thank J.H. and S.R.B. for technical assistance.

Disclosure

None of the authors has any conflict of interest to disclose. We confirm that we have read the Journal's position on issues involved in ethical publication and affirm that this report is consistent with those guidelines.

References

Benbadis SR, LaFrance WC Jr, Papandonatos GD, Korabathina K, Lin K, Kraemer HC. (2009) Interrater reliability of EEG-video monitoring. *Neurology* 73:843–846.

Blanco JA, Stead M, Krieger A, Viventi J, Marsh WR, Lee KH, Worrell GA, Litt B. (2010) Unsupervised classification of high-frequency oscillations in human neocortical epilepsy and control patients. *J Neurophysiol* 104:2900–2912.

Blanco JA, Stead M, Krieger A, Stacey W, Maus D, Marsh E, Viventi J, Lee KH, Marsh R, Litt B, Worrell GA. (2011) Data mining neocortical high-frequency oscillations in epilepsy and controls. *Brain* 134: 2948–2959.

Bragin A, Wilson CL, Staba RJ, Reddick M, Fried I, Engel J Jr. (2002) Interictal high-frequency oscillations (80–500 Hz) in the human epileptic brain: entorhinal cortex. *Ann Neurol* 52:407–415.

Brown MW 3rd, Porter BE, Dlugos DJ, Keating J, Gardner AB, Storm PB Jr, Marsh ED. (2007) Comparison of novel computer detectors and human performance for spike detection in intracranial EEG. *Clin Neurophysiol* 118:1744–1752.

Chatillon CE, Zelmann R, Bortel A, Avoli M, Gotman J. (2011) Contact size does not affect high frequency oscillation detection in intracerebral EEG recordings in a rat epilepsy model. *Clin Neurophysiol* 122:1701–1705.

Davis TS, Parker RA, House PA, Bagley E, Wendelken S, Normann RA, Greger B. (2012) Spatial and temporal characteristics of V1 microstimulation during chronic implantation of a microelectrode array in a behaving macaque. *J Neural Eng* 9:065003.

Hochberg LR, Serruya MD, Friehs GM, Mukand JA, Saleh M, Caplan AH, Branner A, Chen D, Penn RD, Donoghue JP. (2006) Neuronal ensemble control of prosthetic devices by a human with tetraplegia. *Nature* 442:164–171.

Lathi BP. (2005) *Linear systems and signals*. Oxford University Press, New York.

Le Van Quyen M, Staba R, Bragin A, Dickson C, Valderrama M, Fried I, Engel J. (2010) Large-scale microelectrode recordings of high-frequency gamma oscillations in human cortex during sleep. *J Neurosci* 30:7770–7782.

McAdams ET, Jossinet J, Subramanian R, McCauley RG. (2006) Characterization of gold electrodes in phosphate buffered saline solution by impedance and noise measurements for biological applications. *Conf Proc IEEE Eng Med Biol Soc* 1:4594–4597.

Normann RA. (2007) Technology insight: future neuroprosthetic therapies for disorders of the nervous system. *Nat Clin Pract Neurol* 3: 444–452.

Quiroga RQ, Reddy L, Kreiman G, Koch C, Fried I. (2005) Invariant visual representation by single neurons in the human brain. *Nature* 435: 1102–1107.

Schevon CA, Trevelyan AJ, Schroeder CE, Goodman RR, McKhann G Jr, Emerson RG. (2009) Spatial characterization of interictal high frequency oscillations in epileptic neocortex. *Brain* 132:3047–3059.

Schevon CA, Goodman RR, McKhann G Jr, Emerson RG. (2010) Propagation of epileptiform activity on a submillimeter scale. *J Clin Neurophysiol* 27:406–411.

Schevon CA, Weiss SA, McKhann G Jr, Goodman RR, Yuste R, Emerson RG, Trevelyan AJ. (2012) Evidence of an inhibitory restraint of seizure activity in humans. *Nat Commun* 3:1060.

Staba RJ, Wilson CL, Bragin A, Fried I, Engel J Jr. (2002) Quantitative analysis of high-frequency oscillations (80–500 Hz) recorded in human epileptic hippocampus and entorhinal cortex. *J Neurophysiol* 88:1743–1752.

Stacey WC, Kellis S, Patel PR, Greger B, Butson CR. (2012) Signal distortion from microelectrodes in clinical EEG acquisition systems. *J Neural Eng* 9:056007.

Stead M, Bower M, Brinkmann BH, Lee K, Marsh WR, Meyer FB, Litt B, Van Gompel J, Worrell GA. (2010) Microseizures and the spatiotemporal scales of human partial epilepsy. *Brain* 133:2789–2797.

Truccolo W, Donoghue JA, Hochberg LR, Eskandar EN, Madsen JR, Anderson WS, Brown EN, Halgren E, Cash SS. (2011) Single-neuron dynamics in human focal epilepsy. *Nat Neurosci* 14:635–641.

Van Gompel JJ, Stead SM, Giannini C, Meyer FB, Marsh WR, Fountain T, So E, Cohen-Gadol A, Lee KH, Worrell GA. (2008) Phase I trial: safety and feasibility of intracranial electroencephalography using hybrid subdural electrodes containing macro- and microelectrode arrays. *Neurosurg Focus* 25:E23.

Wong S, Gardner AB, Krieger AM, Litt B. (2007) A stochastic framework for evaluating seizure prediction algorithms using hidden Markov models. *J Neurophysiol* 97:2525–2532.

Worrell GA, Jerbi K, Kobayashi K, Lina JM, Zelmann R, Le Van Quyen M. (2012) Recording and analysis techniques for high-frequency oscillations. *Prog Neurobiol* 98:265–278.

Supporting Information

Additional Supporting Information may be found in the online version of this article:

Figure S1. Example of movement artifact in human iEEG.